Charge Solitons in One-Dimensional Arrays of Serially Coupled Josephson Junctions

(Phys. Rev. B **54**, 1234 (1996))

Ziv Hermon[(1)], Eshel Ben-Jacob[(2)], Gerd Schön[(1)]

[(1)]Institut für Theoretische Festkörperphysik, Universität Karlsruhe, D-76128 Karlsruhe, Germany
[(2)]School of Physics and Astronomy, Raymond and Beverly Sackler Faculty of Exact Sciences, Tel-Aviv University, Ramat-Aviv, 69978 Tel-Aviv, Israel

Abstract

We study a 1D array of Josephson coupled superconducting grains with kinetic inductance which dominates over the Josephson inductance. In this limit the dynamics of excess Cooper pairs in the array is described in terms of charge solitons, created by polarization of the grains. We analyze the dynamics of these topological excitations, which are dual to the fluxons in a long Josephson junction, using the continuum sine-Gordon model. We find that their classical relativistic motion leads to saturation branches in the I-V characteristic of a ring-shaped array. We then discuss the semiclassical quantization of the charge soliton, and show that it is consistent with the large kinetic inductance of the array. We study the dynamics of a quantum charge soliton in a ring-shaped array biased by an external flux through its center. If the dephasing length of the quantum charge soliton is larger than the circumference of the array, quantum phenomena like persistent current and coherent current oscillations are expected. As the characteristic width of the charge soliton is of the order of $100\,\mu$m, it is a macroscopic quantum object. We discuss the dephasing mechanisms which can suppress the quantum behaviour of the charge soliton.

1 Introduction

Arrays of Josephson junctions in 1D (one dimension), 2D or 3D have been studied extensively in recent years, both theoretically and experimentally [1]. When the capacitance of the junctions is small, the arrays are usually characterised by the Josephson energy, $\sum_i E_J[1-\cos(\phi_i-\phi_{i+1})]$, and by the charging energy, $\frac{1}{2}\sum_{ij} Q_i C_{ij}^{-1} Q_j$. Here ϕ_i and Q_i denote the phase and the

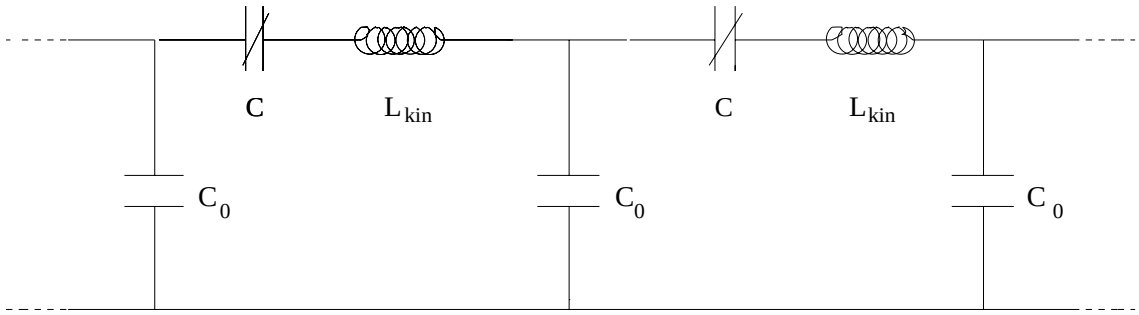

Figure 1: An equivalent electric circuit of a 1D array of serially coupled Josephson junctions.

charge on the ith grain of the array, respectively, C_{ij}^{-1} is the inverse capacitance matrix, and E_J is the Josephson coupling energy. This description in terms of variables defined on the grains and not on the junctions is consistent with the fact that the kinetic and the geometric inductances of the grains are typically smaller than the Josephson inductance. As a result, the charge redistribution time in the grains is shorter than the tunneling time. In this paper we study the opposite limit, namely a 1D array where the kinetic inductance of the grains

$$L_{\rm kin} = \frac{m_e^* l_x}{e^{*2} n_s S} \ , \tag{1}$$

dominates over the Josephson inductance

$$L_J = \frac{1}{(2\pi)^2} \frac{\Phi_0^2}{E_J} \ . \tag{2}$$

Here m_e^* and e^* are the mass and the charge of a Cooper pair, respectively, n_s the Cooper pair density, l_x the length of a grain, and S the cross section of a grain. As we show below this limit is experimentally accessible. However, to the best of our knowledge, this kind of array has not been constructed yet. The large kinetic inductance means that in this case the charge redistribution time in the grains is longer than the tunneling time, thus the dynamic variables should be defined on the junctions of the array and not on the grains. This array can be represented by the electric circuit shown in Fig. 1. C_0 denotes the self-capacitance of the superconducting grains, while the combined effect of the Josephson and charging energies of the junctions results in a nonlinear capacitance, C, as we explain in the next section. We show that in this kind of array the concept of 'charge soliton' [2]-[8] arises, i.e., an excess Cooper pair in the array gives rise to a compact topological solitonic excitation. This appears to be in contrast to the usual model which does not incorporate the inductive effects. That model suggests that an excess Cooper pair delocalises as a consequence of the Josephson tunneling. We show, however, that a sufficiently large kinetic inductance decouples the individual junctions quantum mechanically. We study the dynamics of the charge soliton both classically and quantum mechanically.

The paper is organised as follows: In section (2) we develop a continuum approximation of a serially coupled array of Josephson junctions with a dominant kinetic inductance. In section (3) we show that this array has compact solitonic excitations ('charge solitons'), and discuss some of their classical properties and dynamics. In this section we discuss the small amplitude oscillations of the array ('plasmons') as well. In section (4) we study the classical dynamics of the charge soliton further, using collective coordinates. The quantization of the charge soliton is done in section (5). We discuss the meaning of the semi-classical quantization of the soliton, and study its quantum dynamics in a ring-shaped array. We demonstrate that quantum charge solitons can, in principle, exhibit quantum phenomena without classical analogues, like persistent motion in response to an external flux and coherent current oscillations. We then discuss possible dephasing mechanisms of charge solitons, and address the effects caused by the discreteness of the array. We summarize our results in the concluding section (6).

2 Kinetic Inductance Dominated 1D Array of Serially Coupled Josephson Junctions

2.1 The Lagrangian

We consider a chain of N identical superconducting grains (thus forming $N-1$ Josephson junctions). The junctions are characterised by the Josephson coupling energy and by the charging energy scale

$$E_C \equiv \frac{(2e)^2}{2C} \ . \tag{3}$$

We assume that $C \approx 10^{-15}\,\mathrm{F}$, and that E_J is of the same order as E_C. The grains are capacitively coupled to a conducting substrate with a capacitance $C_0 \ll C$, which we assume to be $C_0 \approx 10^{-17}\,\mathrm{F}$. The energy scale of this coupling energy,

$$E_{C_0} \equiv \frac{(2e)^2}{2C_0} \ , \tag{4}$$

is thus much larger than the junction charging energy

$$E_{C_0} \gg E_C \ . \tag{5}$$

The grains are characterised by the inductive energy scale associated with L_{kin}

$$E_L \equiv \frac{\Phi_0^2}{2L_{\mathrm{kin}}} \ , \tag{6}$$

where $\Phi_0 \equiv h/2e$. As we have said in the introduction, we assume that the kinetic inductance of the grain dominates over the Josephson inductance. In fact, due to the numerical coefficient $(2\pi)^2/2$ difference in the relations

(2) and (6), $L_{\rm kin}$ should be larger than $2\pi^2 L_J$ for the inductive effects to be important. For a typical E_J of the order of $100\,\mu$eV it means that $L_{\rm kin}$ dominates if it is $10^{-7}\,$H or larger. This situation can be achieved, for instance, when $l_x \approx 10\,\mu$m and $S \approx 10^3\,$nm^2. Nevertheless we assume that the width of the grains is of the order of the London penetration depth to avoid tunneling of flux quanta through the grains. The width of the junctions, d, is much smaller than l_x (typically $d \approx 2\,$nm), and the distance between adjacent grains (the unit cell) is denoted by a ($a \equiv l_x + d \approx l_x$). $L \equiv Na$ is the total length of the chain. We assume that the chain is very long ($N \gg 1$).

Using the values given above, we find that the impedance of the array, considered as a transmission line,

$$Z_{LC} = \sqrt{L_{\rm kin}/C_0}\ , \tag{7}$$

is of the order of $100\,$KΩ, i.e. it is much larger than the quantum resistance, $R_Q \equiv h/(2e)^2$:

$$Z_{LC} \gg R_Q\ . \tag{8}$$

Note that this impedance inequality can be expressed alternatively as an inequality of the coupling energy and the inductive energy scales

$$E_{C_0} \gg E_L\ . \tag{9}$$

A similar condition to (8) has been studied before in the context of single electron tunneling in a normal junction [9], and it has been shown that it leads to a quantum mechanical decoupling of the junction from its environment. Using the same reasoning here, we are led to the conclusion that condition (8) means that each junction is quantum mechanically decoupled from its environment, i.e., from the other junctions of the array. We can thus solve the Schrödinger equation for each junction separately, and obtain a local potential energy of the array. This situation has been named the 'local rule' in the context of single electron tunneling [10].

The eigenstates of the junction i depend on $\tilde{q}_i$, the dimensionless charge (in units of $2e$) induced on this junction. As a function of $\tilde{q}_i$, the energy levels are made of a set of charging energy parabolas, with gaps at the intersection regions due to the Josephson energy [11]-[14] (see Fig. 2). The energy levels are, thus, periodic functions of $\tilde{q}_i$ with a period 1. Under appropriate conditions (not too small gaps, adiabatic changes) Zener transitions between the levels can be avoided [15], [16]. We also ignore, for the time being, quasiparticle tunneling, which is a dissipative process. We discuss this issue in section (5). We thus may consider only the first level, which we denote by $E_{\tilde{q}_i}$. This level represents coherent superposition of charge states in the bulk superconductors, which differ by one Cooper pair. $E_{\tilde{q}_i}$ is formally given as an eigenvalue of Mathieu's equation. As it does not have a simple analytical form when E_C is of the same order of E_J, and our results do not depend qualitatively on the exact form of $E_{\tilde{q}_i}$, we adopt the following form

$$E_{\tilde{q}_i} = \frac{2}{(2\pi)^2} E_C[1 - \cos(2\pi\tilde{q}_i)]\ . \tag{10}$$

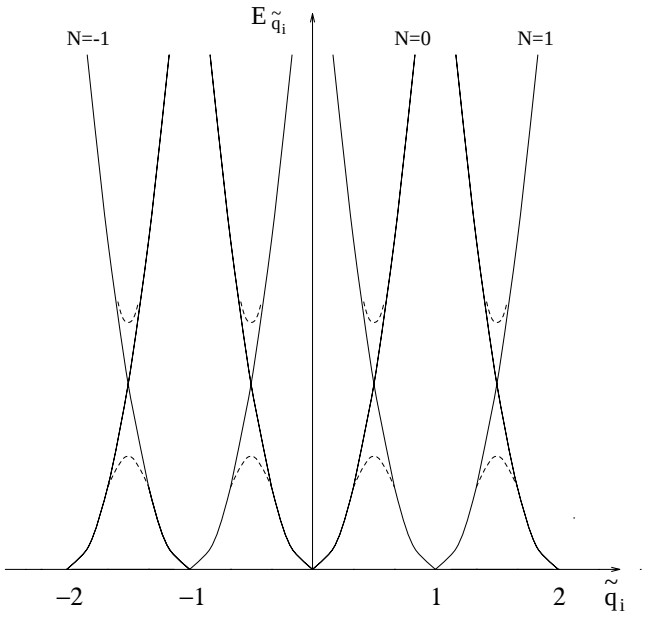

Figure 2: Energy levels of a Josephson junction as a function of $\tilde{q}_i$ for the case $E_J \approx E_C$.

The form (10) preserves the correct parabolic dependence for small q_i, and reduces the amplitude of the energy level from its maximal height (in the limiting case where $E_J = 0$) by a factor of $\pi^2/4$. We emphasize that the important feature of $E_{\tilde{q}_i}$ is its periodicity, which allows us to represent the Josephson junction as a nonlinear capacitor (see Fig. 1). In the next section we show that the periodicity gives rise to the soliton description.

Due to the tunneling of Cooper pairs the variable $\tilde{q}_i$ is compact, i.e. $\tilde{q}_i + 1 = \tilde{q}_i$. It is convenient to introduce an extended variable q_i, which is the dimensionless charge (in units of $2e$) brought to the ith junction. q_i is related to $\tilde{q}_i$ through

$$q_i \equiv \tilde{q}_i + \sum_{i'=i+1}^{N} Q_{i'} \ , \tag{11}$$

where Q_i is the net charge on the ith *grain*. Q_i has, of course, only discrete values, while q_i and $\tilde{q}_i$ are continuous. This change of variables corresponds to changing from a 'reduced zone' scheme to an 'extended zone' scheme in the junction's energy bands (see Fig. 2). This variable was used in the study of 1D arrays of serially coupled normal junction as well [2], [4]. In the next section we show the importance of q_i for the solitonic description. The form of the energy of the junction (the potential energy) does not change when expressed as a function of q_i

$$E_{\rm pot} = E_{q_i} = \frac{2}{(2\pi)^2} E_C [1 - \cos(2\pi q_i)] \ . \tag{12}$$

The voltage across the junction, V_{q_i}, is given by the derivative of the energy

levels with respect to the charge

$$V_{q_i} = \frac{1}{2e}\frac{\partial E_{q_i}}{\partial q_i} \ . \tag{13}$$

Using (12) we express the voltage as

$$V_{q_i} = \frac{1}{2\pi} V_C \sin(2\pi q_i) \ , \tag{14}$$

where $V_C \equiv \frac{2e}{C}$.

Since q_i is defined on the junction it is already contains an averaging over the fast tunneling process. A time dependent q_i is therefore related to the slow process of charge redistribution in the grains by means of a supercurrent. This gives rise to an inductive energy in the grains, which serves as the kinetic energy of the array:

$$E_{\rm kin} = \frac{1}{2}(2e)^2 L_{\rm kin} \dot{q}_i^2 \ . \tag{15}$$

In the parameters range we consider, the kinetic energy scale is smaller than the potential energy one:

$$E_C > E_L \ . \tag{16}$$

The three inequalities, (5), (9) and (16) can be combined into a single condition for the energy scales of the system:

$$E_{C_0} > E_C > E_L \ . \tag{17}$$

The relation between the dynamic variable q_i and the voltage V_i between the ith grain and the substrate can be found by consecutive applications of Gauss' law:

$$q_i = q_1 - \frac{1}{2e} C_0 \sum_{i'=1}^{i} V_{i'} \ , \tag{18}$$

where q_1 is the charge that was brought to the first junction of the array. From now on we assume that the continuum limit can be taken. (We will show the necessary condition for this soon.) Discreteness effects are discussed in section (5). In the continuum limit Eqs. (11) and (18) have the form

$$q(x) \equiv \tilde{q}(x) + \int_x^L Q(\xi)\, d\xi/a \ , \tag{19}$$

$$q(x) = q(0) - \frac{1}{2e} C_0 \int_0^x V(\xi)\, d\xi/a \ . \tag{20}$$

The array is thus described by the charge field $q(x)$. Relation (20) between $q(x)$ and $V(x)$ can be expressed in a local form

$$V(x) = -a\frac{2e}{C_0} q_x(x) \ . \tag{21}$$

We see that the $q_x(x)$ is the dimensionless charge between the grains and the substrate. The charging energy which couples the unit cells of the array can be expressed, therefore, as

$$E_{\rm coupling} = a^2 \frac{(2e)^2}{2C_0} q_x^2 \ . \tag{22}$$

As we have mentioned above, its energy scale is E_{C_0} (4). Since $C_0 \ll C$ we have $E_{C_0} \gg E_C$. In this case even small amounts of charge induce high voltages on the capacitors between the grains and the substrate, and these voltages strongly couple the Josephson junctions. In the opposite case, when C_0 is large, there is almost no voltage on the capacitors and the junctions are practically decoupled. A small C_0 is thus needed for the picture of serially coupled Josephson junctions.

From the above discussion we conclude that the array we consider is characterised by the three energies: the potential energy (12), the kinetic (or inductive) energy (15) and the coupling (or charging) energy (22). When these three energies are combined, we get the following sine-Gordon Lagrangian

$$\mathcal{L} = \frac{1}{2a}(2e)^2 L_{\rm kin} \dot{q}^2 - a\frac{(2e)^2}{2C_0} q_x^2 - \frac{1}{a}\frac{2}{(2\pi)^2}\frac{(2e)^2}{2C}[1-\cos(2\pi q)] \ . \tag{23}$$

This is a novel description of a 1D Josephson junctions array, which is valid when condition (17) holds. The three effects of the large kinetic inductance are reflected in the Lagrangian (23): 1. an additional inductive energy, which is an inertial term; 2. a representation of each junction by a periodic charging energy, as a result of the quantum mechanical decoupling of the junctions; 3. a description of the array by degrees of freedom which are defined on the junctions and not on the grains. The Lagrangian (23) is electromagnetically dual to the Lagrangian representing a long Josephson junction. The latter system can be understood as the continuum version of an array of parallely coupled Josephson junctions. Interchanging parallel coupling with series coupling and inductors with capacitors one gets the Lagrangian of the serially coupled Josephson junctions. Note, especially that the periodic inductive energy in the long Josephson junction (i.e., the Josephson energy) is replaced here by the periodic charging energy.

2.2 The Equation of Motion and the Hamiltonian

Following the standard sine-Gordon treatment [17], [18], we redefine the charge field: $q(x) \to q'(x) \equiv q(x)/2\pi$, and express the Lagrangian (23) as

$$\mathcal{L} = \frac{\hbar v_C}{2\pi\beta^2}\left[\frac{1}{2v_C^2}\dot{q}^2 - \frac{1}{2}{q_x}^2 - \frac{1}{\Lambda_C^2}(1-\cos q)\right] \ . \tag{24}$$

The three bulk parameters: C, $L_{\rm kin}$ and C_0 are replaced in (24) by Λ_C, v_C and β^2. Here

$$\Lambda_C \equiv a\sqrt{\frac{C}{C_0}} \ , \tag{25}$$

is the characteristic length of the system. The condition needed for the validity of the continuum limit is therefore

$$\Lambda_C \gg a \ , \tag{26}$$

or

$$C \gg C_0 \ , \tag{27}$$

which is consistent with the limit (5). This is another manifestation of what we have discussed above: a small C_0 implies a large coupling, hence a large Λ_C. Using the values given above we get $\Lambda_C \approx 100\,\mu$m. The second parameter in the Lagrangian (24),

$$v_C \equiv \frac{a}{\sqrt{L_{\rm kin} C_0}} \ , \tag{28}$$

is the wave velocity of the system. It is of the order of $10^{-1} - 10^{-2}\,c$, where c is the vacuum light velocity. It is related to Λ_C via the characteristic frequency

$$\omega_C = \frac{v_C}{\Lambda_C} = \sqrt{\frac{1}{L_{\rm kin} C}} \ , \tag{29}$$

which is of the order of $10^{11}\,\sec^{-1}$. The third parameter in the Lagrangian (24),

$$\beta^2 \equiv \frac{2\pi\hbar v_C C_0}{(2e)^2 a} \ , \tag{30}$$

sets the energy scale of the system. It does not affect the classical equation of motion, but its value is important in determining whether the system behaves classically or quantum mechanically. We return to this point in section (5), where we discuss the quantum dynamics of the system.

The equation of motion derived from the Lagrangian (24) is

$$\frac{1}{v_C^2}\ddot{q} - q_{xx} + \frac{1}{\Lambda_C^2}\sin q = 0 \ . \tag{31}$$

It is a voltage equation for the junction, as can be shown more clearly by multiplying it by $2ev_C^2 L_{\rm kin}/2\pi$ and using Eq. (21) to obtain

$$\frac{1}{2\pi} 2eL_{\rm kin}\ddot{q} - \frac{1}{2\pi} a^2 \frac{2e}{C_0} q_{xx} + \frac{1}{2\pi} V_C \sin q = 0 \ . \tag{32}$$

The first term is an inductive voltage induced along the grains when the current is time dependent. From Eq. (21) we see that the second term is the continuum form of $V_{i+1} - V_i$, i.e., it is the difference of the voltages between two adjacent cells and the substrate. The third term is the voltage across the junctions, resulting from the superposition of charge states (Eq. (14)). The voltage equation (32) is thus a Kirchoff's law for a closed loop

of the equivalent electrical circuit of the array (see Fig. 1). The conjugate momentum of the field q

$$\pi_q \equiv \frac{\partial \mathcal{L}}{\partial \dot{q}} = \frac{1}{a}\left(\frac{2e}{2\pi}\right)^2 L_{\rm kin}\dot{q} \equiv \hbar\tilde{n}_{\Phi_0} \ , \tag{33}$$

is the number of flux quanta per unit length that have tunneled through the junctions of the array. Using $\tilde{n}_{\Phi_0}$ we get the Hamiltonian of the system

$$H = \hbar v_C \int \left\{ 2\pi\beta^2 \frac{1}{2}\tilde{n}^2_{\Phi_0} + \frac{1}{2\pi\beta^2}\left[\frac{1}{2}q_x^2 + \frac{1}{\Lambda_C^2}(1-\cos q)\right]\right\} dx \ . \tag{34}$$

When the array is coupled to an external voltage, $V_{\rm ext}$, the equation of motion (31) changes to

$$\frac{1}{v_C^2}\ddot{q} - q_{xx} + \frac{1}{\Lambda_C^2}\sin q = 2\pi\frac{1}{a^2}\frac{C_0}{2e}V_{\rm cell} \ , \tag{35}$$

where

$$V_{\rm cell} \equiv \frac{a}{L}V_{\rm ext} \tag{36}$$

is the part of the external voltage that is distributed on one unit cell. Equation (35) represents, alternatively, the case where the array has a shape of a ring and an external flux is applied through its center. In this case $V_{\rm ext} \equiv -\dot{\Phi}_{\rm ext}$ is the electromotiv force acting on the array. The flux source has, of course, the advantage that the effects of the leads are eliminated. In any case, Eq. (35) can be derived from the following Hamiltonian

$$H = \hbar v_C \int \left\{ 2\pi\beta^2 \frac{1}{2}(\tilde{n}_{\Phi_0} - \tilde{n}_{\Phi_{\rm ext}})^2 + \frac{1}{2\pi\beta^2}\left[\frac{1}{2}q_x^2 + \frac{1}{\Lambda_C^2}(1-\cos q)\right]\right\} dx \ . \tag{37}$$

In the case of a voltage source $\tilde{n}_{\Phi_{\rm ext}}$ is defined as the integral of the external voltage per unit length and unit flux

$$\tilde{n}_{\Phi_{\rm ext}} \equiv -\frac{1}{L\Phi_0}\int V_{\rm ext}\, dt \ , \tag{38}$$

while in the case of a flux source it is simply the dimensionless flux density. The external source thus appears in the Hamiltonian as a time dependent gauge potential, in analogy to the external current in the long Josephson junction Hamiltonian [19]. The gauge nature of the external voltage gives rise to the following shift of the conjugate momentum

$$\hbar\tilde{n}_{\Phi_0} = \frac{1}{a}\left(\frac{2e}{2\pi}\right)^2 L_{\rm kin}\dot{q} + \hbar\tilde{n}_{\Phi_{\rm ext}} \ . \tag{39}$$

Dissipation processes in the system produce additional q-dependent voltage drops. Ohmic dissipation can be represented phenomenologically by

adding to each unit cell a resistor connected to the other elements in this cell in series. In this case the voltage equation (35) becomes

$$\frac{1}{v_C^2}\ddot{q} + \frac{1}{a^2}C_0 R\dot{q} - q_{xx} + \frac{1}{\Lambda_C^2}\sin q = 2\pi\frac{1}{a^2}\frac{C_0}{2e}V_{\rm cell} \ . \tag{40}$$

This representation, which was named the 'serially resistive junction' (SRJ) in Ref. [2], is the analogue of the RSJ model [20], [21].

3 Charge Solitons and Plasmons

3.1 A Static Charge Soliton

Since the 1D array of serially coupled Josephson junctions can be described by a sine-Gordon Lagrangian (24), we expect that it has solitonic excitations, i.e., compact, stable topological configurations. Using the definition of q as an extended variable (19), we observe that $q(x)$ and $q(x+2\pi)$ can be distinguished if there is an excess or a deficiency of Cooper pairs in intermediate grains. The one-soliton excitation represents the charging of the junctions (or the polarization of the grains) due to an excess Cooper pair in the array, and is called a 'charge soliton'. This term was coined in Ref. [2] in the context of a 1D array of normal tunnel junctions. Recently, charge solitons in a 1D array of SQUID's (Superconducting QUantum Interference Device) have been studied experimentally [8], and a zero current state below a threshold voltage was found. This voltage was interpreted as an injection voltage for a charge soliton.

The charge soliton solution of Eq. (31) with the appropriate boundary conditions is (see Fig. 3 (a))

$$q_{\rm sol}(x) = 4\tan^{-1}\left[\exp\left(\frac{x-X_0}{\Lambda_C}\right)\right] - 2\pi \ . \tag{41}$$

Its center is at X_0, which we take in this section to be zero. The excess charge of the Cooper pair is the topological charge of this soliton

$$Q = \frac{2e}{2\pi}\int \partial_x q_{\rm sol}\, dx = -2e \ . \tag{42}$$

We would like to emphasize once more that under the conditions we consider here, the existence of a topological solitonic excitation and its stability do not depend on the exact form of the potential energy of the junctions, but only on its having degenerate minima. Thus our qualitative results are valid for other forms of the potential as well.

As was mentioned above, charge solitons in 1D arrays of normal tunnel junctions have been studied previously [2]-[7]. In this context a question was raised whether a charge soliton can be regarded as a coherent dynamic object whose equation of motion contains an inertial term, as was proposed in Refs.

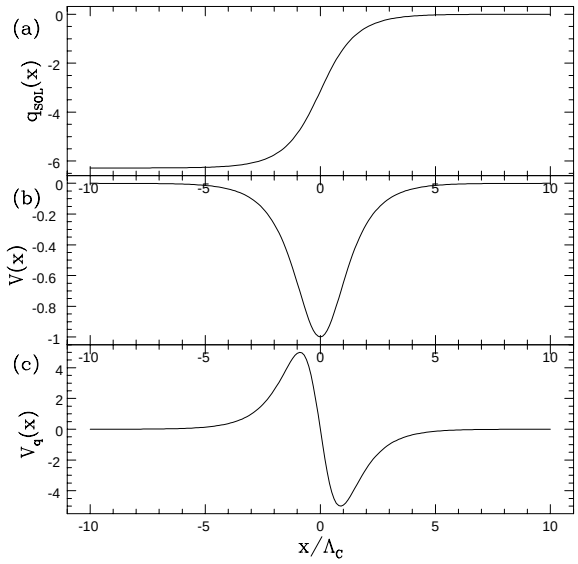

Figure 3: (a) The charge soliton configuration representing an excess Cooper pair in the array. The center of the soliton is taken to be $X_0 = 0$. (b) The profile of the voltage between the array and the substrate induced by the charge soliton. V is measured in mV. (c) The distribution of voltages on the junctions of the array corresponding to a charge soliton configuration. V_q is measured in mV.

[2], [3] and [4], or that it merely represents a static charge distribution profile, as was argued in Refs. [5] and [6]. Here we have shown that this question should not rise in the Josephson junction array context. The coherence of the charge soliton ensues from the coherent superconducting ground state, and the inertia term comes from the kinetic inductance of the grains. Moreover, we have shown that the impedance condition (8) should be met in order that the concept of a charge soliton will be different from that of a point charge (be it a Cooper pair or an electron).

From Eq. (41) we see that the characteristic length scale of the array, Λ_C, is the characteristic width of the soliton as well. In order to interpret the charge soliton as a particle its width should be much smaller than the total length of the array, i.e.,

$$L \gg \Lambda_C \ . \tag{43}$$

This assumption is met when $L \geq 10^3\,\mu$m. Here we assume that $L \approx 10^3\,\mu$m. The number of grains the soliton is spread over is

$$N_C \equiv \Lambda_C/a = \sqrt{C/C_0} \ . \tag{44}$$

N_C is larger than one due to the continuum limit condition (26). For the parameters given above $N_C = 10$. When condition (26) fails, one should take

into account corrections to the continuum sine-Gordon model. We address this point in section (5). The finite width of the charge soliton is clearly seen from its density, which according to Eq. (21), is proportional to the profile of the voltage between the array and the substrate (see Fig. 3 (b))

$$V(x) = -\frac{a}{2\pi}\frac{2e}{C_0}\partial_x q_{\rm sol}(x) = -\frac{2}{2\pi}\frac{1}{N_C}\frac{2e}{C_0}{\rm sech}\left(\frac{x}{\Lambda_C}\right) \ . \tag{45}$$

Λ_C sets the scale for the static distribution of voltages on the junctions of the array as well. Using Eqs. (14) and (31) we find that this distribution is proportional to the second derivative of the soliton configuration (see Fig. 3 (c))

$$V_q(x) = \frac{1}{2\pi}V_C\Lambda_C^2\,\partial_{xx}q_{\rm sol}(x) = -\frac{2}{2\pi}V_C\ {\rm sech}\left(\frac{x}{\Lambda_C}\right)\tanh\left(\frac{x}{\Lambda_C}\right) \ . \tag{46}$$

The energy needed to create a charge soliton is the value of the Hamiltonian calculated for a static solution (Eq. (41))

$$E_0 = \frac{8}{\Lambda_C}\frac{\hbar v_C}{2\pi\beta^2} = \frac{8}{(2\pi)^2}\frac{(2e)^2}{\sqrt{CC_0}} = \frac{16}{(2\pi)^2}E_C N_C \ . \tag{47}$$

This rest energy depends on C and C_0 but not on $L_{\rm kin}$, since it is determined by the potential and coupling energies. It can be written as the potential energy density ($\epsilon_C \equiv E_C/S$), times the effective area of the soliton ($S_{\rm eff} \equiv SN_C$)

$$E_0 = \frac{16}{(2\pi)^2}\epsilon_C S_{\rm eff} \ . \tag{48}$$

Dividing Eq. (47) by v_C^2 we get the soliton rest mass

$$M_0 \equiv E_0/v_C^2 = \frac{8}{(2\pi)^2}(2e)^2\frac{L_{\rm kin}}{a}\frac{1}{\Lambda_C} \ . \tag{49}$$

In analogy to the rest mass of a fluxon in a long Josephson junction [19], the charge soliton's rest mass is proportional to the inductance per unit length and inversely proportional to the characteristic length, Λ_C. Using the typical parameters we find that the charge soliton mass is of the order of 10^{-36} Kg, i.e. six orders of magnitude less than the electron rest mass. This result indicates that the charge soliton should not be understood as a Cooper pair dressed with a polarization cloud, but as the polarization cloud itself. We return to this point when we discuss the dynamics of the charge soliton in the next section.

3.2 A Dynamic Soliton

In order to describe a charge soliton moving with a velocity v, we make use of the Lorentz invariance of the Lagrangian (24) to perform a Lorentz transformation of the static configuration (41) and obtain

$$q_{\rm sol}(x,t) = q_{\rm sol}[\gamma(x-vt)] = 4\tan^{-1}\left\{\exp\left[\gamma\left(\frac{x-x_0-vt}{\Lambda_C}\right)\right]\right\} - 2\pi \ , \tag{50}$$

where $\gamma \equiv 1/\sqrt{1-(v^2/v_C^2)}$. We thus expect that a relativistic charge soliton suffers a Lorentz contraction. Since the light velocity in the array, v_C, is smaller than the vacuum light velocity, relativistic effects of the charge soliton can be observed more easily than relativistic effects of electrons or Cooper pairs.

A moving charge soliton induces, of course, a current along the array. The spatial distribution of the current is given by

$$I(x,t) = \frac{2e}{2\pi}\dot{q}_{\rm sol}(x,t) \ . \tag{51}$$

This is a current pulse with a width Λ_C, concentrated around the moving center of the charge soliton. It has the same profile as the voltage between the array and the substrate (see Fig. 3 (b)). The average current produced by the moving soliton is

$$\bar{I} = \frac{1}{L}\int I(x)\,dx = -\frac{1}{L}2ev \ . \tag{52}$$

For a soliton moving with a velocity 10^6 m/sec, it is of the order of 0.1 nA.

3.3 Plasmons

Besides topological solitons, the sine-Gordon Lagrangian (24) admits small amplitude excitations. Their dynamics is governed by the linearized equation of motion

$$\frac{1}{v_C^2}\ddot{q} - q_{xx} + \frac{1}{\Lambda_C^2}q = 0 \ . \tag{53}$$

As this equation describes electromagnetic field oscillations with a confining potential, its solutions are longitudinal plasma oscillations ('plasmons') propagating along the array. The propagation of the plasmons does not involve any tunneling process. The plasmons have the dispersion relation

$$\omega^2 = \omega_C^2 + v_C^2 k^2 \ , \tag{54}$$

i.e., there is an energy gap $\hbar\omega_C$ in their spectrum with the corresponding temperature $T_g \approx 1\,{\rm K}$. The plasmons have, therefore, a mass

$$M_P = \frac{\hbar\omega_C}{v_C^2} = \frac{\hbar}{\Lambda_C v_c} \ , \tag{55}$$

which is of the order of 10^{-37} Kg. The ratio between the mass of a plasmon to the mass of the soliton (49) is $2\pi\beta^2/8$, i.e., it is of the order of β^2.

Plasmons can also be excited when there is a soliton in the array. In that case they can be considered as vibrations of the soliton. Their analytical form is

$$\psi_k(x) \sim \left[\tanh\left(\frac{x}{\Lambda_C}\right) - ik\Lambda_C\right]\exp(ikx) \ . \tag{56}$$

The dispersion relation is the same as above (Eq. (54)), but there exists now an additional zero mode (whose $\omega = 0$). It reflects the translational invariance of the system, i.e., the homogeneity of the array (at distances larger than a).

4 Collective Coordinates for the Charge Soliton

4.1 Equations of motion and the Dynamic Mass

The topological stability of the charge soliton and its finite width allow for its interpretation as a particle. Thus we would like to describe the charge soliton by a pair of conjugate coordinates which correspond to its center of mass, X, and to its momentum, P. This can be done by using the 'collective coordinates' method. This method was studied extensively in the context of general soliton theory [22]-[25], as well as for long Josephson junctions in particular [2], [4], [19], [26], [27]. We assume that the form of the charge soliton is

$$q(x,t) = q_{\rm sol}(x - X(t)) \ , \tag{57}$$

i.e., that it is a rigid object moving with a velocity $\dot{X}$. This assumption means that we neglect the effects of the plasmons. It is justified when the temperature is much lower than the plasmons' energy gap.

The collective coordinates can be expressed in an explicit form [27]:

$$X \equiv -\frac{1}{2\pi} \int x \partial_x q_{\rm sol} \, dx \ , \tag{58}$$

$$P \equiv \int \pi_q \partial_x q_{\rm sol} \, dx \ . \tag{59}$$

Inserting the soliton configuration (50) into definitions (58) and (59) we get the equations of motion of a free relativistic particle

$$X = X_0 + vt \ , \tag{60}$$

$$\dot{X} = v \ , \tag{61}$$

$$P = \gamma M_0 \dot{X} \ , \tag{62}$$

$$\dot{P} = 0 \ . \tag{63}$$

The mass that appears in (62) is actually the dynamic mass of the charge soliton

$$M_d \equiv -\frac{1}{a} \left(\frac{2e}{2\pi} \right)^2 L_{\rm kin} \int \partial_x q_{\rm sol}^2 \, dx \ . \tag{64}$$

Its value is identical to the rest mass (49) in the limit $L \gg \Lambda_C$, and differs from it by a factor of 2 in the opposite limit $L \ll \Lambda_C$. As we consider here the first limit, we denote it by M_0 as well. We can understand the origin

of the dynamic mass by observing the way the charge soliton propagates. Starting from the static distribution of voltages on the junctions (see Fig. 3 (c)), the center of the charge soliton moves from its position in the middle of a grain towards one of the neighbouring junctions, say the right one, by a charge redistribution in the grains. A superposition of charge states in the two adjacent grains is built, and the (negative) voltage on this junction is reduced. When the superposition is of states of equal weight, the voltage is zero. As the motion continues, the charge redistribution increases the weight of the charge state on the right grain and the voltage on the junction is increased. When the absolute value of this voltage reaches the initial one, the center of the charge soliton has been shifted by one unit cell, i.e., it is in the middle of the right grain. One sees that the propagation of the charge soliton is determined by the kinetic inductance and not by the Josephson one. The dynamic mass leads us, therefore, to the same conclusion that we got from the rest mass: the charge soliton is the polarization cloud that accompanies the excess Cooper pair that exists in the array.

Transforming now the Hamiltonian (34) into collective coordinates form, we get

$$H = \sqrt{M_0^2 v_C^4 + P^2 v_C^2} \ , \tag{65}$$

so the energy of the moving soliton is

$$E = \gamma M_0 v_C^2 = \gamma E_0 \ . \tag{66}$$

If we assume the nonrelativistic limit, i.e., $v \ll v_c$, the Hamiltonian describing the soliton as a particle reads

$$H = M_0 v_C^2 + \frac{P^2}{2M_0} \ , \tag{67}$$

where now

$$P = M_0 \dot{X} \ . \tag{68}$$

The rest energy term in the Hamiltonian (67) is made out of the two charging energies (the last two terms in (34)), while the contribution to the kinetic term in (67), comes only from the inductive energy (the first term in (34)). We thus see that the inductive energy, although being the smallest energy in the system, is the one that governs the dynamics of the charge soliton. The independence of the Hamiltonian (67) on X is another manifestation of the translation invariance of the system.

4.2 A Voltage Biased Array

The collective coordinates can be used to describe a voltage (or a time varying flux) biased array as well. Introducing the external voltage in the form

$$\dot{\Phi}_{\rm ext} \equiv -V_{\rm ext} \ , \tag{69}$$

we find that the collective momentum is shifted to

$$P = M_0 \dot{X} + \frac{2\pi\hbar}{L}\frac{\Phi_{\rm ext}}{\Phi_0} \ , \tag{70}$$

and the nonrelativistic particle Hamiltonian is

$$H = M_0 v_C^2 + \frac{1}{2M_0}\left(P - \frac{2\pi\hbar}{L}\frac{\Phi_{\rm ext}}{\Phi_0}\right)^2 \ . \tag{71}$$

The equations of motion derived from (71) are

$$\dot{X} = \frac{1}{M_0}\left(P - \frac{2\pi\hbar}{L}\frac{\Phi_{\rm ext}}{\Phi_0}\right) \ , \tag{72}$$

and

$$\dot{P} = 0 \ . \tag{73}$$

Combining the two equations we get

$$M_0 \ddot{X} = -\frac{2\pi\hbar}{L}\frac{\dot{\Phi}_{\rm ext}}{\Phi_0} \ , \tag{74}$$

i.e., the external voltage accelerates the charge soliton without changing its momentum. The origin of this acceleration is simply the electrostatic force exerted on the excess Cooper pair by the external voltage. In order that the rigid soliton assumption will be valid in this case as well, the external flux must be changed adiabatically, or the external voltage should be small enough,

$$\left|\frac{\dot{\Phi}_{\rm ext}}{\Phi_0}\right| = \left|\frac{V_{\rm ext}}{\Phi_0}\right| \ll \omega_C \ , \tag{75}$$

which means that $V_{\rm ext}$ should be of the order of $10\,\mu$V or less.

When there are Ohmic dissipation processes in the array an application of an external voltage results in a steady state velocity (or current) of the soliton. Using the Hamiltonian (34), the equation of motion (40), and the average current (52), we find that the steady state condition is

$$V_{\rm ext} = R_{\rm eff}\bar{I}_{\rm steady} \ , \tag{76}$$

where the effective resistance of the array is constant in the nonrelativistic case

$$R_{\rm eff} \equiv \frac{8}{(2\pi)^2}\frac{L^2}{a\Lambda_C}R \tag{77}$$

and is $\bar{I}_{{\rm ea}steady}$ dependent in the relativistic case

$$R_{\rm eff,\,rel}(\bar{I}_{\rm steady}) \equiv \frac{8}{(2\pi)^2}\frac{L^2}{a\Lambda_C}\gamma(\bar{I}_{\rm steady})R \tag{78}$$

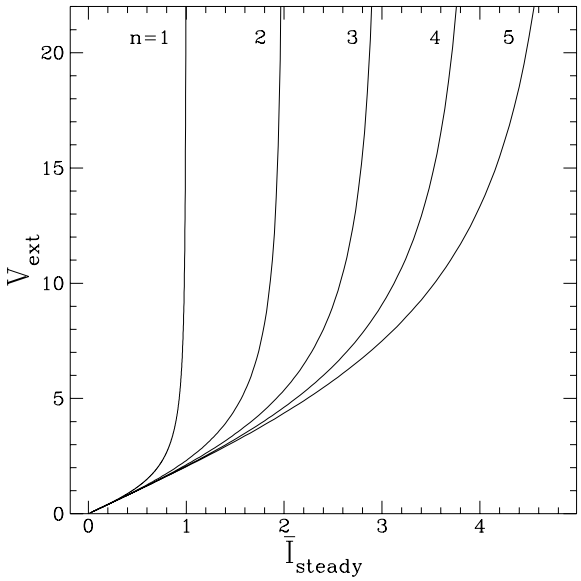

Figure 4: I-V characteristic of a ring-shaped dissipative array biased by a time varying flux ($V_{\rm ext} \equiv -\dot{\Phi}_{\rm ext}$ is the electromotiv force produced by the flux). Each branch corresponds to a certain number of charge solitons in the system. $V_{\rm ext}$ is measured in μV and $\bar{I}_{\rm steady}$ is measured in nA. The parameters are $R = 10\Omega$ and $v_C = 10^{-2}c$.

The effective nonrelativistic resistance of the array is thus increased by about two orders of magnitude, while relativity increases it further by the γ factor. Relation (76) between the external voltage and the steady state current is dual to the relation between the external current biasing a long Josephson junction and the steady state voltage a moving fluxon creates [26], [28]. The I-V characteristic of the array is expected to show saturation branches, where each branch corresponds to a certain number of solitons reaching the limit velocity, v_C (see Fig. 4). These branches are expected to be observed in a ring-shaped array, since charge solitons can enter and leave an open array in a continuous manner.

5 Quantum Dynamics of the Charge Soliton

5.1 The Semi-Classical Expansion

In this section we study the quantum dynamics of the charge soliton as a particle. For this we utilise the semi-classical quantization of the sine-Gordon theory [17], [18], [22], [29]. The expansion parameter is the coupling constant β^2, which was defined in (30). In this method the total Fock space is taken to be composed of disconnected sectors, each one corresponds to different topological boundary conditions, i.e., to a different number of solitons in the system. The ground state of each sector is the corresponding solitonic

configuration. Here we concentrate on the one-soliton sector. Due to the translational invariance of the system there is, in fact, a degenerate family of eigenstates of the position operator, connected by space translations. Higher states are found by a semi-classical expansion around the ground state. The excitations of the first order correspond to the plasmons, and their quantum interpretation is as light particles scattering from the static massive soliton. These plasmons are, thus, the fundamental quanta of the theory. The degeneracy of the states is completely removed in the second order, as the position eigenstates are replaced by momentum eigenstates, and the translation invariance of the theory is recovered on the quantum level. The semi-classical expansion breaks down when $\beta^2 \geq 2$, where the soliton becomes lighter than the plasmons. The soliton then takes the role of the fundamental quantum, and loses its correspondence to the classical particle configuration (in a sense it becomes 'too' quantum). Since the typical value of β^2 is 10^{-1}, we can use the expansion for the array. The parameter β^2 can be expressed in the form [30]

$$\beta^2 = \sqrt{\frac{E_L}{E_{C_0}}} = \frac{R_Q}{Z_{LC}} \ . \tag{79}$$

Comparing Eq. (79) with (8) and (9), we see that the condition for using the semi-classical expansion, $\beta^2 \ll 1$, is identical to the impedance condition. This is not a surprise, as the impedance condition is the one that enables us to decouple the junctions quantum mechanically. Our model of the charge soliton as a classical configuration is thus self-consistent.

However there are several differences between the system we study and the field theoretical model. First of all, the array is very long (compare to Λ_C), but finite. Apart from a slight distortion to the soliton's shape that we neglect, the finiteness means that solitons can enter and leave the array, and also get reflected from the edges. To avoid this situation, we consider a ring-shaped array. Second, since the gap in the plasmons' spectrum is of the order of one Kelvin, their population can be made negligible if the temperature is kept below the gap. Thus we can discard all the plasmons' contribution to the dynamics. This assumption is equivalent to the rigid soliton assumption (57). A finite population of plasmons can be considered as an internal environment which produces a phase breaking mechanism [31]. We comment on this dephasing process at the end of this section. Another different feature is that we couple the array to an external (classical) flux source as a gauge coupling, and study the quantum dynamics of the soliton in response to this source. Finally, the array we study deviates from the ideal sine-Gordon model by its discreteness, by the exact form of the potential energy, by structural inhomogeneities and disorder, and by quasiparticle tunneling. The effects of these deviations from the ideal model are discussed below.

5.2 Persistent Motion of the Charge Soliton

In the presence of an external flux, $\Phi_{\rm ext}$, the assumption of rigidity leads to the following nonrelativistic quantum Hamiltonian for a ring-shaped array of serially coupled Josephson junctions:

$$\hat{H} = M_0 v_C^2 + \frac{1}{2M_0}\left(\hat{P} - \frac{2\pi\hbar}{L}\frac{\Phi_{\rm ext}}{\Phi_0}\right)^2 \ . \tag{80}$$

Higher order contributions to the energy give rise to quantum corrections to the soliton's rest mass [32]. The renormalized mass in the array language (up to the order of β^0) is

$$M_{0\,\rm ren} = \frac{8}{\Lambda_C}\frac{\hbar}{2\pi\beta^2 v_C}\left(1 - \frac{\beta^2}{4}\right) = M_0\left(1 - \frac{\beta^2}{4}\right) \ . \tag{81}$$

However since β^2 is small we can use M_0 instead of $M_{0\,\rm ren}$. As we have discussed in the previous section, the Hamiltonian is $\hat{X}$ independent due to the homogeneity of the array. Thus it commutes with the collective momentum operator, $\hat{P}$, and the eigenstates are collective momentum eigenstates with a discrete set of eigenvalues, $p_N = \hbar k_N$ determined by the periodic boundary conditions

$$k_N = \frac{2\pi\hbar}{L}N\,; \qquad N = 0, \pm 1, \pm 2, ... \quad . \tag{82}$$

The energy spectrum is discrete, too, and is given by (neglecting the constant term $M_0 v_C^2$)

$$E_N = \frac{1}{2M_0}\left(\frac{2\pi\hbar}{\Phi_0 L}\right)^2 (\Phi_0 N - \Phi_{\rm ext})^2 \ . \tag{83}$$

Defining an effective inductance by

$$L_{\rm eff} \equiv \left(\frac{\Phi_0 L}{2\pi\hbar}\right)^2 M_0 \tag{84}$$

($L_{\rm eff} \approx 10^{-5}$ H), the energy levels can be expressed in the form of inductive levels

$$E_N = \frac{1}{2L_{\rm eff}}(\Phi_0 N - \Phi_{\rm ext})^2 \ . \tag{85}$$

The inductive form of the energy levels suggests the interpretation of N as the number of flux quanta that have tunneled outside or inside the ring through one of the junctions. The quantization of $\hat{P}$ is, therefore, the statement that only an integral number of flux quanta can tunnel in or out of the ring. However, the conservation of the momentum means that there can be no flux tunneling in an homogeneous array, i.e., the external flux is completely screened.

The spectrum of the charge soliton's Hamiltonian (83) is periodic with respect to the external flux with a period Φ_0. It is composed of a set of parabolas centered at $\Phi_{\rm ext} = N\Phi_0$. Each parabola intersects its two adjacent

parabolas at $(N+1/2)\Phi_0$ (see Fig. 5). The current along the array is given by

$$\langle \hat{I} \rangle = -\frac{\partial E_N}{\partial \Phi_{\rm ext}} = \frac{1}{L_{\rm eff}}(\Phi_0 N - \Phi_{\rm ext}) \ . \tag{86}$$

It is proportional to the expectation value of the velocity of the charge soliton

$$\langle \dot{\hat{X}} \rangle = \frac{L}{2\pi\hbar}\frac{\partial E_N}{\partial N} = \frac{L}{2e}\langle \hat{I} \rangle \ . \tag{87}$$

This is the quantum version of relation (52). We see that the external flux induces a persistent motion of the charge soliton, which is manifested in a persistent current along the array. As was shown above, no net number of flux quanta can tunnel in or out of the junction. However, during the motion of the soliton one can think of flux quanta flowing in and out of the array through the junctions, thus forming a flux loop around the moving center of the soliton. (A similar idea for 2D superconducting films was given in Ref. [33].) This interpretation is dual to the interpretation of the fluxon in a long Josephson junction as a (charge) current loop. The charge soliton's persistent current has the same origin as the persistent current of electron in a metal ring [34]. It is a manifestation of the Aharonov-Bohm effect [35] of a charged particle encircling a flux tube, and its persistency is due to the particle being in an exact eigenstate of the system. However, in contrast to the electron, the charge soliton is a macroscopic particle ($\Lambda_C \approx 100\,\mu$m), so the possibility that it exhibits quantum effects is very intriguing. The quantum behaviour of the charge soliton is dual to the quantum behaviour of the fluxon in a long Josephson junction [19]. The latter exhibits a persistent motion in response to an external bias charge, which is the manifestation of the Aharonov-Casher effect [36]. Being a magnetic particle, this motion results in a persistent voltage across the junction.

A weak spatial inhomogeneity in the array, e.g., nonidentical grains or junctions or disordered grains, gives an additional $\hat{X}$-dependent term in the Hamiltonian (80). The momentum is not conserved anymore, and flux quanta can tunnel across the array, reflecting in the spectrum by gaps which are opened at the intersection points of the parabolas (see Fig. 5). If the array is now adiabatically biased by a time varied flux source, the persistent current oscillates as a function of $\Phi_{\rm ext}$ with a period Φ_0. In each period a flux quantum tunnels across the array. This tunneling creates a current in the inverse direction to the existing current, thus eliminating the net current and reducing the energy. Since the energy bands are exact eigenstates, the tunneling process is a coherent one. When the external flux is not equal to an integral number of flux quanta, the quantum state of the array is a superposition of two flux quantum states. The amplitude of a persistent current of one charge soliton decreases as the amount of inhomogeneity increases. The maximal amplitude, corresponding to a vanishing amount of inhomogeneity, is of the order of 0.1 nA.

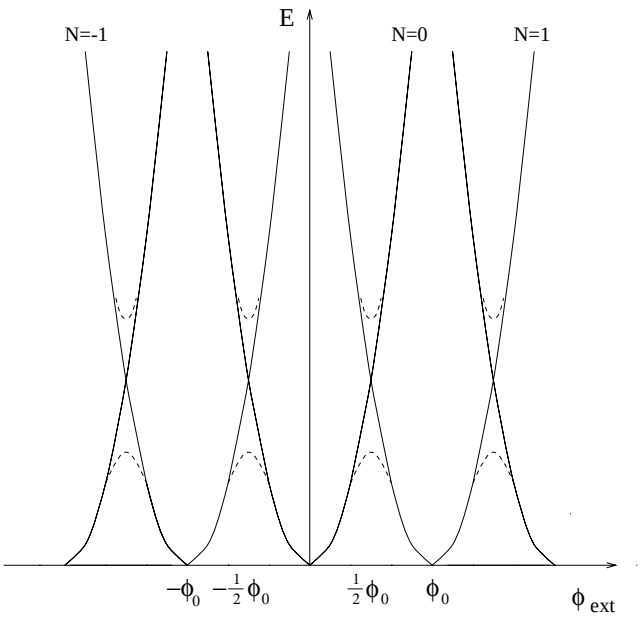

Figure 5: The spectrum of a quantum charge soliton in a 1D ring-shaped array of serially coupled Josephson junctions as a function of an external flux, $\Phi_{\rm ext}$. In an ideal ring the spectrum consists of inductive energy parabolas without a possibility of crossing at the intersection points. When there is some inhomogeneity in the ring (e.g., due to disorder), gaps are open at the intersection points, and the spectrum develops into energy bands.

5.3 Other Quantum Effects

The quantum nature of the charge soliton can be revealed in transport phenomena as well. For instance, if solitons are sent through a ring-shaped array connected to two leads (all consist of serially coupled Josephson junction), and the dephasing mechanisms are suppressed, we expect that they will split into partial waves propagating along the two arms of the ring. The partial waves will then interfere at the outgoing leads, with the interference pattern being dependent on the length of the arms and on an external flux applied through the center of the ring. The transmission of quantum charge solitons through the ring is thus expected to show oscillations as a function of the external flux and of the optical path similar to the h/e oscillations in the transmission of electrons through a metal ring [37], and in analogy to the transmission of fluxons through a Josephson junction ring [38].

5.4 Dephasing Mechanisms

The quantum phenomena described above were a consequence of the fact that in our approximation the Hamiltonian (80) was a one-particle Hamiltonian. Thus, even in the presence of a weak inhomogeneity, the degree of freedom associated with the charge soliton's center of mass (X_0) can maintain its quantum coherence. In order to make the model more realistic, one

should take into account interactions between the soliton and other degrees of freedom. These interactions can produce, in principle, phase breaking mechanisms. Whenever the phase breaking length, defined as the length over which the soliton's phase has an uncertainty of 2π, is smaller than the length of the array, the quantum phenomena exhibited by the charge soliton will be suppressed. As in the case of the fluxon in a long Josephson junction [31], we can distinguish between internal and external dephasing mechanisms. The internal mechanism is due to the interaction between the charge soliton and the other degrees of freedom of the junction, i.e., the plasmons. When the sine-Gordon model is exact and continuous, the system is completely integrable and the soliton is decoupled from the plasmons. Nevertheless, it has been shown in the context of the fluxon in a long Josephson junction [31] that there is a possibility of dephasing in this case as well. In order to avoid this dephasing, the temperature should be below the plasmons' energy gap. In the context of the charge soliton, where the sine-Gordon model is only an approximation and the system is discrete, we expect that the plasmons give rise to a stronger dephasing due to their inelastic interaction with the soliton. From the study of the discrete sine-Gordon model it is known that the rest energy of a soliton whose center resides in a junction is higher than the rest energy for a soliton whose center resides in the middle of a grain [39], [40]. Thus the soliton propagates in a periodic potential and not in a flat one. This deviation from the continuum model produces a coupling between the plasmons and the soliton. The soliton can emit or absorb plasmons [39], [40], and the circulating soliton can become phase locked with this plasmons [41]. This effect has been recently observed for the fluxon in the discrete long Josephson junction [42]. We expect that similar phenomena occur in the system we study here when the continuum condition (26) does not hold. Apart from producing a phase breaking length, these phenomena will affect the classical dynamics as well, for instance by creating resonances in the I-V characteristic. The influence of both the discreteness of the array and the deviation from the exact sine-Gordon model on the classical and quantum mechanical dynamics of the charge soliton should be studied further.

The most important external dephasing mechanisms are due to interaction with quasiparticles, which was neglected in our model. Since the bulk superconductors energy gap, Δ, is typically of the same order or higher than the plasmons' energy gap, the condition needed to suppress the thermal activation of the plasmons is sufficient to suppress the thermal activation of the quasiparticles. The effects of thermal quasiparticles will be studied elsewhere. The quasiparticles can destroy the quantum coherence of the array in another way, which is temperature independent. The complete spectrum of a single junction includes charging energy parabolas associated with quasiparticles as well, which are separated in the charge axis by e. Excitation of quasiparticles leads to transitions between these parabolas, thus destroying the quantum coherence of q. This effect can be neglected if the charging energy of the quasiparticles plus the superconducting energy gap is larger than the Cooper

pairs charging energy, i.e., $2\Delta + e^2/8C > e^2/2C$ or $(32/3)\Delta > E_C$. Since E_C should be smaller than Δ for the existence of the Josephson effect, this condition is met automatically.

6 Summary

We have studied a 1D array of serially coupled Josephson junctions in the limit when the kinetic inductance of the superconducting grains dominates over the Josephson inductance. In this case the array is described by variables which are defined on the junctions and not on the grains. We have shown that the large kinetic inductance decouples the junctions quantum mechanically. As a result each junction is characterised by a periodic charging energy. This periodic energy, when combined with the inductive energy of the grains and the charging energy between the grains and the substrate, gives rise to a model with topological solitons excitations. Thus we have found that an excess Cooper pair in the array creates a charge soliton via polarization of the superconducting grains. The charge soliton is a dual topological excitation to the fluxon in a long Josephson junction. We have studied the classical dynamics of the charge soliton, and shown that in the presence of dissipation and an external time varying flux the I-V characteristic of a ring-shaped array should consist of saturation branches corresponding to the number of charge solitons in the array. We have quantized the charge soliton semiclassically, showing that this quantization is consistent with the large kinetic inductance. We have found that a quantum soliton in a flux-biased ring-shaped array is expected to show persistent motion, manifested in a persistent current. A weak inhomogeneity in the array gives rise to a coherent current oscillations. These phenomena, which are usually associated with electrons (or Cooper pairs) suggests that the quantum charge soliton can be considered as a macroscopical quantum object. Finally, we have discussed possible internal and external dephasing mechanisms of the charge soliton. These mechanisms deserve future study.

Acknowledgments: We like to thank G. D. Guttman, A. Shnirman, D. B. Haviland, P. Delsing, R. Fazio, F. Guinea, A. V. Ustinov, B. A. Malomed and S. E. Korshunov for very fruitful discussions. One of us (Z.H.) is supported by the MINERVA fellowship. This research was supported in part by the Wolfson Foundation via the Israeli Academy of Sciences, and by the DFG within the research program of the Sonderforschungbereich 195.

References

[1] For a number of articles see the *Proceedings of the NATO Advanced Research Conference on Mesoscopic Superconductivity*, edited by F. W. J. Hekking, G. Schön and D. V. Averin (North Holland, Amsterdam, 1994); and the *Proceedings of the NATO Advanced Research Conference on Quantum Dynamics of Submicron Structures*, edited by

H. A. Cerdeira, B. Kramer and G. Schön (Kluwer Academic Publishers, Dordrecht, 1995), and references therein.

[2] E. Ben-Jacob, K. Mullen and M. Amman, Phys. Lett. A **135**, 390 (1989).

[3] M. Amman, E. Ben-Jacob and K. Mullen, Phys. Lett. A **142**, 16 (1989).

[4] M. Amman, E. Ben-Jacob and Z. Hermon, in *Single Electron Tunneling and Mesoscopic Devices*, edited by H. Koch and H. Lübbig (Springer-Verlag, Berlin, 1992).

[5] K. K. Likharev, N. S. Bakhvalov, G. S. Kazacha and S. I. Serdyukova, IEEE Trans. Magn. **25**, 1436 (1989).

[6] N. S. Bakhvalov, G. S. Kazacha, K. K. Likharev and S. I. Serdyukova, Zh. Eksp. Teor. Fiz. **95**, 1010 (1989) [Sov. Phys. JETP **68**, 581 (1989)].

[7] P. Delsing, in *Single Charge Tunneling*, edited by H. Grabert and M. H. Devoret (Plenum Press, New York, 1992).

[8] D. B. Haviland and P. Delsing, unpublished.

[9] M. H. Devoret, D. Esteve, H. Grabert, G.-L. Ingold, H. Pothier and C. Urbina, Phys. Rev. Lett. **64**, 1824 (1990); S. M. Girvin, L. I. Glazman, M. Jonson, D. R. Penn and M. D. Stiles, *ibid.* **64**, 3183 (1990).

[10] U. Geigenmüller and G. Schön, Europhys. Lett. **10**, 765 (1989).

[11] A. Widom. G. Megaloudis, T. D. Clark, H. Prance and R. J. Prance, J. Phys. A **15**, 3877 (1982).

[12] E. Ben-Jacob and Y. Gefen, Phys. Lett. **108A**, 289 (1985).

[13] K. K. Likharev and A. B. Zorin, J. Low Temp. Phys. **59**, 347 (1985).

[14] G. Schön and A. D. Zaikin, Phys. Rep. **198**, 237 (1990).

[15] E. Ben-Jacob, Y. Gefen, K. Mullen and Z. Schuss, in *SQUID'85*, edited by H. D. Hahlbohm and H. Lübbig (de Gruyter, Berlin, 1985).

[16] E. Ben-Jacob, Y. Gefen, K. Mullen and Z. Schuss, Phys. Rev. B **37**, 7400 (1988).

[17] S. Coleman, *Aspect of Symmetry* (Cambridge University Press, Cambridge, 1985), Chap. 6.

[18] R. Rajaraman, *Solitons and Instantons* (North-Holland, Amsterdam, 1982).

[19] Z. Hermon A. Stern and E. Ben-Jacob, Phys. Rev. B **49**, 9757 (1994).

[20] D. E. McCumber, J. Appl. Phys. **39**, 3113 (1968).

[21] W. C. Stewart, Appl. Phys. Lett. **12**, 277 (1968).

[22] N. H. Christ and T. D. Lee, Phys. Rev. D **12**, 1606 (1975).

[23] J. L. Gervais and B. Sakita, Phys. Rev. D **11**, 2943 (1975).

[24] R. Rajaraman and E. Weinberg, Phys. Rev. D **11**, 2950 (1975).

[25] E. Tomboulis, Phys. Rev. D **12**, 1678 (1975).

[26] D. W. McLaughlin and A. C. Scott, Phys. Rev. **18A**, 1652 (1978).

[27] D.J. Bergman, E. Ben-Jacob, Y. Imry and K. Maki, Phys. Rev. **27A**, 3345 (1983).

[28] P. M. Marcus and Y. Imry, Solid State Commun. **33**, 345 (1980).

[29] R. Jackiw, Rev. Mod. Phys. **49**, 681 (1977).

[30] Z. Hermon, Ph.D. thesis, Tel-Aviv University.

[31] Z. Hermon, A. Shnirman and E. Ben-Jacob, Phys. Rev. Lett. **74**, 4915 (1995).

[32] R. Dashen, B. Hasslacher and A. Neveu, Phys. Rev. D **10**, 4130 (1974); **11**, 3424 (1975).

[33] M-C. Cha, M. P. A. Fisher, S. M. Girvin, M. Wallin and A. P. Young, Phys. Rev. B **44**, 6883 (1991).

[34] M. Büttiker, Y. Imry and R. Landauer, Phys. Lett. **96A**, 365 (1983).

[35] Y. Aharonov and D. Bohm, Phys. Rev. **115**, 485 (1959).

[36] Y. Aharonov and A. Casher, Phys. Rev. Lett. **53**, 319 (1984).

[37] Y. Gefen, Y. Imry and M. Ya. Azbel, Phys. Rev. Lett. **52**, 129 (1984).

[38] A. Shnirman, Z. Hermon, L. Vaidman and E. Ben-Jacob, Phys. Rev. A **52**, 3541 (1995).

[39] J. F. Currie, S. E. Trullinger, A. R. Bishop and J. A. Krumhansl, Phys. Rev. B **15**, 5567 (1977).

[40] M. Peyrard and M. D. Kruskal, Physica D **14**, 88 (1984).

[41] A. V. Ustinov, M. Cirillo and B. A. Malomed, Phys. Rev. B **47**, 8357 (1993).

[42] H. S. J. van der Zant, T. P. Orlando, S. Watanabe and S. H. Strogatz, Phys. Rev. Lett. **74**, 174 (1995).